

Article

Study on a Correlation-Based Anti-Islanding Method under Wider Frequency Trip Settings for Distributed Generation

Byunggyu Yu 

Kongju National University, Gongju-si 330-717, Korea; bgyuyu@kongju.ac.kr; Tel.: +82-41-521-9162

Received: 29 April 2020; Accepted: 22 May 2020; Published: 24 May 2020

**Featured Application:** Grid Connected Inverter.

Abstract: Islanding phenomenon of distributed generation (DG), such as photovoltaic (PV) generation, is undesirable because it causes safety issues for utility service personnel and power system equipment. Many anti-islanding methods have been studied since DG appeared in electric power systems (EPSs). Most anti-islanding methods focus on disconnecting DG from the grid using functionality to detect islanding under narrow frequency trip settings, because safety issues have a higher priority. However, as DG plays a key part of an EPS, a significant loss of DG due to a short disturbance could result in a reliability issue for the EPS. Corresponding to this matter, new international standards, such as IEEE standard 1547–2018, require more sophisticated and complex functionalities for grid-connected DGs by adopting ride-through technologies and wider voltage/frequency trip settings. Since most anti-islanding functions of inverter-based DG have been based on the frequency of the inverter voltage, it is more difficult to detect islanding under wider frequency trip settings. This paper presents a correlation-based anti-islanding method (AIM) without depending on the frequency trip of inverter-based DGs. Simulation results are provided to verify the performance of the correlation-based anti-islanding method. As a result, the proposed method detects islanding at 0.116 s under wider frequency trip setting by the IEEE Std. 1547–2018 test condition, while the popular active frequency drift method with positive feedback does not detect islanding using the same current disturbance.

Keywords: anti-islanding; distributed generation; grid-connection; photovoltaic generation; frequency trip setting

1. Introduction

Distributed generation (DG) based on renewable energy resources provides power to local loads in coordination with the main power grid [1–3]. DG is now commonly installed in electric power systems (EPSs) [4]. At present, EPSs have become increasingly complex in terms of their operation and controls because of the significant penetration of DGs [5]. The islanding phenomenon of DG has been regarded as one of the major issues of increased DGs in EPSs. Islanding is defined as a condition in which a portion of the utility with a DG and load remains energized even though that portion is disconnected from the remainder of the utility system, as shown in Figure 1 [6]. Since islanding causes safety issues for both utility service personnel and power system equipment, it is desirable that it is prevented [7]. However, as the utilization of DG has increased rapidly in EPSs, a possible significant loss of DG due to a short disturbance could potentially aggravate the problem and cause a wide-spread blackout.

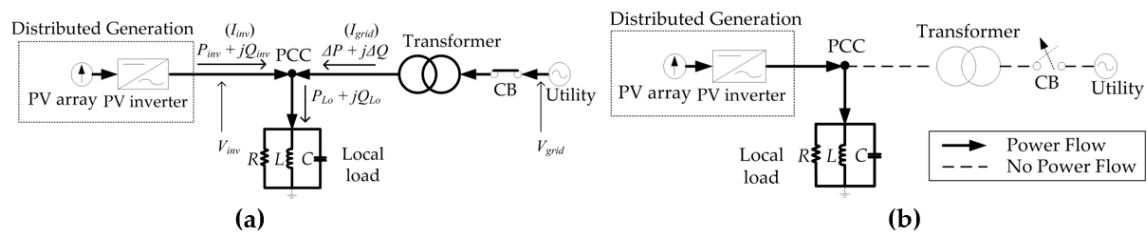


Figure 1. Description of islanding phenomenon: (a) grid-connected mode; (b) islanding mode.

As a result of this issue, new requirements for grid-connected technology, including ride-through and anti-islanding technology, which are more sophisticated and complex, have been recently proposed [8,9]. According to these new requirements, ride-through is the ability to withstand voltage and frequency disturbances, whereas trip is the cessation of output without immediate return to service. As trip requirements are related to the islanding of DG, a requirement for anti-islanding within two seconds is applied when DG is isolated from the upstream part of the area EPS. To date, as shown in Figure 2, a variety of anti-islanding methods (AIMs), including local techniques and remote techniques, have been developed and implemented. Remote methods depend on communication techniques between DG and the EPS but tend to be more costly than local methods [10]. Local methods are usually implemented into the grid-connected inverter of DG and they are typically classified as passive and active methods. Passive methods, based on power mismatches between DG power and local loads, detect islanding only by monitoring several system parameters such as voltage magnitude [11], frequency [12], phase jump [13], and harmonic detection [14]. On the other hand, active islanding methods perturb the DG inverter current in order to break the power balance between DG and local loads in the form of frequency drifting [15,16] and reactive power drifting [17,18]. In addition, neural network, pattern recognition and machine learning-based AIMs have been proposed [19,20]. Since most anti-islanding functions of inverter-based DG have been based on the frequency of the inverter voltage, it is more difficult to detect islanding under wider frequency trip settings. To solve this technical barrier, this paper is based on a correlation technique [21].

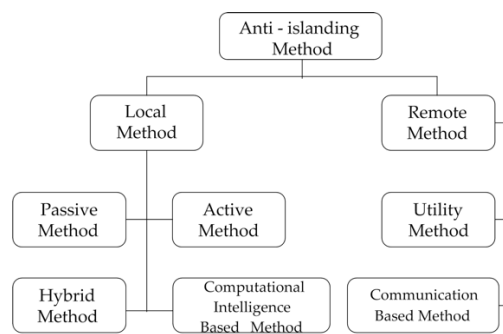


Figure 2. Classification of anti-islanding method.

In this paper, study of a correlation-based AIM under wider frequency trip settings for distributed generation is presented. A non-detection zone (NDZ) by frequency trip settings is analyzed under IEEE Std. 1547–2018, compared with the previous settings under IEEE Std. 1547–2003. Then, a newly proposed correlation-based AIM method is presented with a corresponding simulation for its verification.

2. NDZ Comparisons

In the early days of the dissemination of DG, safe energy generation of the EPS was important. For voltage and frequency variation, which are indicators of EPS accidents such as blackouts, the focus was on disconnecting the DG from the EPS. As DG has been implemented in EPSs with large capacities,

a significant loss of DG due to a short disturbance could cause another reliability issue for the EPS. As a result, new international standards, such as IEEE standard 1547–2018, require more sophisticated and complex requirements for grid-connected DGs. For short voltage and frequency disturbances, the ride-through capability was adopted to continue the operation of DG, as shown in Figure 3. These wider voltage and frequency trip windows allow DG to generate electric power even though there is a slight voltage and frequency disturbance. On the other hand, islanding of DG should be prevented in an EPS because it may cause safety issues. Thus, IEEE Std. 1547–2018 requires islanding detection within 2 s without compromise. However, since most anti-islanding methods are based on frequency trip windows, there have been concerns about the reduced effectiveness of anti-islanding under the new standard requirements.

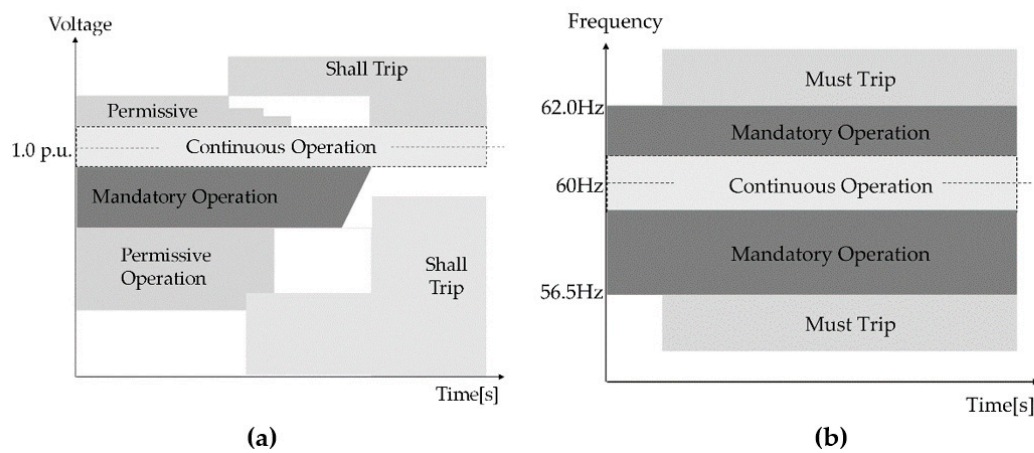


Figure 3. A simplified ride-through capability required in IEEE Std. 1547–2018: (a) voltage ride-through profile; (b) frequency ride-through profile (default setting).

The relationship between reactive power mismatch ΔQ and frequency threshold can be obtained by [22]:

$$Q_f \left[1 - \left(\frac{f}{f_{min}} \right)^2 \right] < \frac{\Delta Q}{P_{inv}} < Q_f \left[1 - \left(\frac{f}{f_{max}} \right)^2 \right] \quad (1)$$

$$Q_f = R \sqrt{\frac{C}{L}} = \frac{\sqrt{|Q_L||Q_C|}}{P_R} \quad (2)$$

where P_{inv} is the active power of the DG inverter; ΔQ is the reactive power flow from the grid; f is the grid frequency; f_{min} and f_{max} are the under and over frequency thresholds, respectively; and Q_f is a quality factor. The quality factor is defined as the measure of the resonance strength of the islanding test load, as shown in Figure 1a [23].

With the limit values of the frequency specified in Table 1, the corresponding NDZ was derived. This quantitative NDZ is the basis to calculate the amount of frequency perturbation of the DG inverter, which causes the harmonic distortion of the current. It has been one of the main research targets for detecting islanding with high power quality and low harmonics.

As shown in Table 1, the islanding test conditions changed to reduce the effect on the EPS by decreasing Q_f from 2.5 to 1. Additionally, the frequency relay settings were changed in a wider direction to prevent nuisance trips. Table 1 shows that NDZ varies by Equation (1) according to the set value of the frequency trip settings and the value of Q_f . Among the NDZ ranges of the three different standards, IEEE Std. 1547–2018 shows the largest NDZ because it has the widest frequency trip settings. Under the wide range of frequency trip settings, the current disturbance command of AIM must increase to make the frequency move out of the range when islanding occurs. Since this disturbance appears as the current distortion, harmonic components increase or displacement power factor decreases, resulting in

poor power quality. Thus, this paper presents a correlation-based AIM that does not depend on the frequency trip.

Table 1. Historical frequency trip settings of the distributed generation (DG) inverter.

Standard	Over Frequency [Hz]	Under Frequency [Hz]	Clearing Time	Condition	Non Detection Zone as $\frac{\Delta Q}{P}$
IEEE Std. 929–2000	60.5	59.3	6 [cycles]	≤ 10 [kW], $Q_f = 2.5$	$-5.94\% \leq \frac{\Delta Q}{P} \leq 4.12\%$
IEEE Std. 1547–2003	60.5	59.3	0.16 [s]	≤ 30 [kW], $Q_f = 1$	$-2.37\% \leq \frac{\Delta Q}{P} \leq 1.65\%$
IEEE Std. 1547–2018	62.0	56.5	0.16 [s]	Default setting, $Q_f = 1$	$-12.77\% \leq \frac{\Delta Q}{P} \leq 6.35\%$

3. The Proposed AIM

As one of the most used AIMs, the active frequency drift (AFD) method with positive feedback has been studied often [24–26]. Accordingly, this method was applicable to be implemented in a commercial photovoltaic (PV) inverter to meet the requirements of IEEE Std. 1547–2003. As shown in Figure 4, the AFD method uses the chopping fraction, cf , as a frequency perturbation parameter, which is defined as the ratio of zero time (t_z) to half of the period of voltage waveform ($T_1/2$) as follows:

$$cf = \frac{t_z}{(T_1/2)} \tag{3}$$

where t_z is zero time of the inverter current and T_1 is a period of voltage waveform.

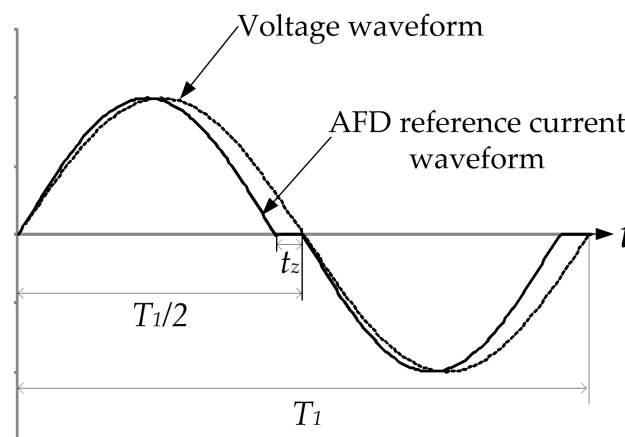


Figure 4. Active frequency drift (AFD) reference current waveform compared with the voltage waveform.

Without the AFD method, the current is controlled to be in phase with the voltage waveform, which results in a unity power factor control. When the AFD method is applied, the frequency of the DG inverter is maintained by the grid voltage when the grid is connected, so there is no frequency variation due to zero time of the AFD reference current. It is important to design an appropriate cf value because harmonic components are generated by the injected AFD current command. When the DG inverter is disconnected from the grid, the AFD current command makes the frequency drift to the frequency trip set value, and the inverter stops [24–26].

If an AFD current disturbance with a fixed cf can be canceled by local load adjustment, the chopping fraction is usually modified with a positive feedback as follows [24]:

$$cf[k] = cf[k - 1] + K_p(Freq[k] - Freq[k - 1]) \tag{4}$$

where k is the present status, K_p is a proportional coefficient, and $Freq$ is the measured frequency of the voltage.

Since the displacement factor (DPF) is 1, the power factor (PF) and the reactive power can be expressed as follows [27]:

$$PF = \frac{P}{S} = \frac{P}{\sqrt{P^2 + Q^2}} = \frac{1}{\sqrt{1 + THD_i^2}} \tag{5}$$

$$\frac{Q}{P} = THD_i \tag{6}$$

Since total harmonic distortion of current (THD_i) is directly proportional to cf , the amount of reactive power variation (Q/P) in Equation (6) can be determined by cf . The previous research showed the relationship between cf and THD_i through some experiments [27]. The allowable limit of THD_i (5%) by the standard sets the maximum cf about 5% [27,28]. In the case of the new IEEE Std. 1547–2018, the amount of perturbation ($\Delta Q/P_{inv}$) increases dramatically, as shown in Table 1. Consequently, a higher cf of the AFD method is required to prevent islanding. Thus, it is difficult to use the conventional AFD with positive feedback (AFDPF) by IEEE Std. 1547–2018 because the corresponding THD_i is around 12.77% which is higher than the standard limit [28]. Since NDZs, as shown in Table 1, are valid only when AIMS depend on the frequency trip settings, this paper presents a novel method using a correlation parameter without depending on the frequency trip settings.

$$C_p[k] = \sum_{n=0}^{n=N} (cf[k - n] - cf[k - n - 1]) \times (freq[k - n] - freq[k - n - 1]) \tag{7}$$

where k is the present status and N is the number of line frequency for C_p calculation.

As shown in Equation (7), this paper presents the correlation parameter C_p as an islanding detection indicator without depending on the frequency trip setting. The proposed method uses the fact that the frequency of the DG inverter voltage has a strong correlation with the current frequency deviation after islanding. As shown in Figure 5, when the grid is connected, the inverter voltage of the DG is dominated by the rigid grid voltage source and has a weak correlation with the proposed AFD frequency perturbation. Thus, C_p is maintained to be almost zero before t_0 . On the other hand, after islanding, C_p starts to increase after t_0 and reaches $C_{p,set}$, and islanding is prevented.

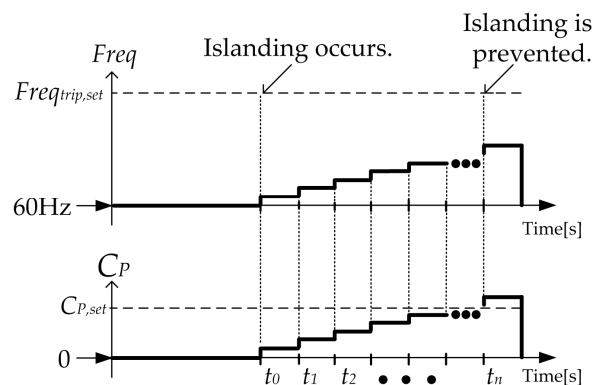


Figure 5. Operational waveform of the proposed anti-islanding method.

For the AFDPF method, the key design parameter of cf is the positive feedback gain K_p , which accelerates cf deviation as frequency changes. K_p was designed and chosen by trial-and-error simulations for short frequency trip settings, 59.3 and 60.5 Hz from IEEE Std. 1547–2003. For IEEE Std. 1547–2018, the frequency trip settings, 56.5 and 62 Hz, are wider. Thus, if AFDPF method is used, K_p for IEEE Std. 1547–2018 should be larger than K_p for IEEE Std. 1547–2003, which increases the harmonic components. In this paper, K_p 0.02, which is designed for 59.3 and 60.5 Hz, is also used to show the feasibility for 56.5 and 62 Hz by using the proposed AIM. In summary, the proposed method does not depend on the frequency trip settings and is based on the correlation between the rate of change of the input current perturbation and the rate of change of the corresponding frequency. This means that islanding can be detected using the proposed correlation parameter with less cf perturbation under IEEE Std. 1547–2018.

4. Simulation Results

The performance of the proposed method was verified using PSIM software under the conditions of IEEE Std. 1547–2018. The key parameters for islanding test are shown in Table 2 and simulation circuit is shown in Figure 6. The local load was chosen as a unity power quality factor for a 3 kW DG inverter system. By adjusting tunable RLC local load, a test condition was implemented for the worst case, the power balance condition between DG generation and local load consumption. The threshold value of the correlation factor was chosen to be 0.0013, which was derived from the value of cf for IEEE Std. 1547–2003. This is to show that the designed cf for IEEE Std. 1547–2003 can also be applied to IEEE Std. 1547–2018 using the proposed method. In other words, the lower cf value, which was designed for IEEE Std. 1547–2003, can be used for IEEE Std. 1547–2018.

Table 2. DG’s key parameters for simulation.

Parameter	Value
Local load R, L, C power	Quality factor $Q_f = 1$ $P_R = 3$ kW $Q_L = 3$ kVar $Q_C = 3$ kVar
Single DG inverter nominal power, P_{inv}	3 kW
Threshold value of correlation parameter, $C_{p,set}$	0.0008 (when $N = 5, K_p = 0.02$)
Frequency trip setting	OF: 62 Hz, UF: 56.5 Hz
OF: 62 Hz, UF: 56.5 Hz	$56.5 < f < 62$ Hz
Nominal grid voltage, frequency, V_{grid}	220 V, 60 Hz single phase

Figure 7 shows islanding test results when no AIM is applied. When the local loads are almost matched with DG power generation and the grid is disconnected at 0.5 s, the measured frequency is almost maintained to be 60 Hz. Thus, islanding is not detected at all. Figure 8 shows anti-islanding test results when the conventional AFD method with 5% cf is used. Before islanding occurs, the inverter output current is clearly distorted by cf , as shown in Figure 8. Once islanding occurs, the frequency of inverter voltage stays still around 60 Hz, because DG source and load power are balanced under the constant cf disturbance. Thus, islanding is not prevented in this case. In the same way, Figure 9 shows anti-islanding test results when AFDPF method is used. Before islanding occurs, it is hard to recognize the distortion of the inverter output current as shown in Figure 9, because the initial value cf for AFDPF method is 1%. After islanding at 0.5 s, the frequency is drifted by cf over 60.5 Hz and then stabilized under 62 Hz. Even though cf is increased by the positive feedback, the frequency variation after islanding is not enough to detect islanding by depending on frequency trip settings. This means that AFDPF method may meet the requirements of anti-islanding under IEEE Std. 1547–2003, whose frequency trip setting is at 60.5 Hz. However, this AFDPF method does not meet the requirement of IEEE Std. 1547–2018 because its frequency trip point is 62 Hz.

Figure 10 shows anti-islanding test results when the proposed method is used. Before islanding occurs, the distortion of the current is small like the AFDPF method since the initial value cf is 1%. In addition, before islanding, the proposed correlation parameter C_P is maintained to be almost zero because frequency is dominated by the rigid grid voltage source, not the chopping fraction. In other words, there is little correlation between cf and frequency before islanding. However, after islanding, the frequency is determined by the chopping fraction with positive feedback. Therefore, the proposed correlation factor starts to increase to be over 0.0013. Therefore, islanding can be prevented by the proposed islanding indicator, C_P .

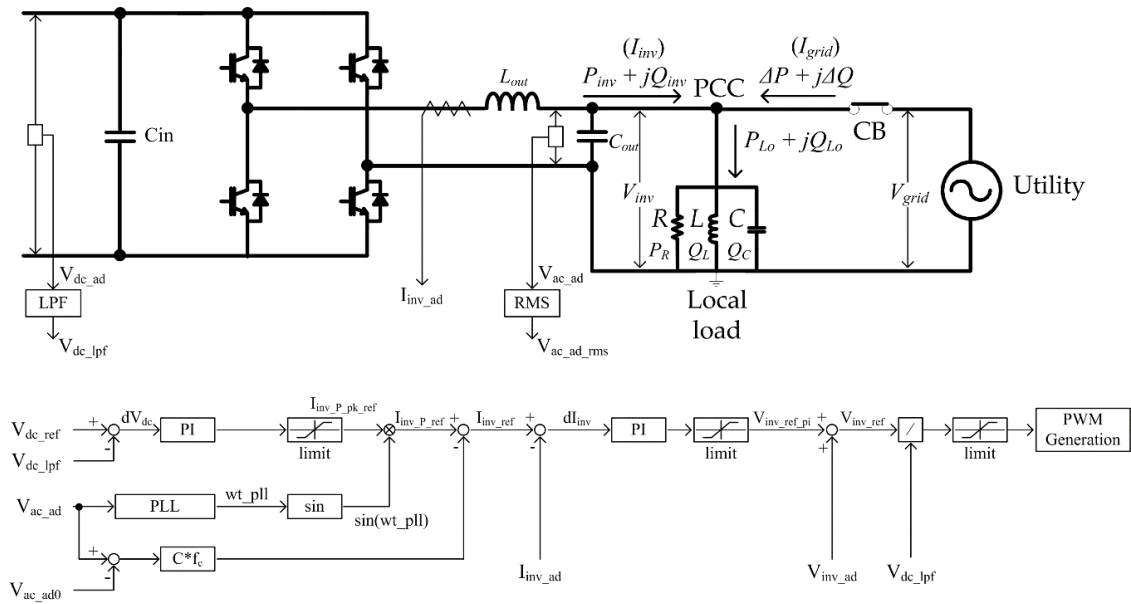


Figure 6. Simulation circuit for islanding test.

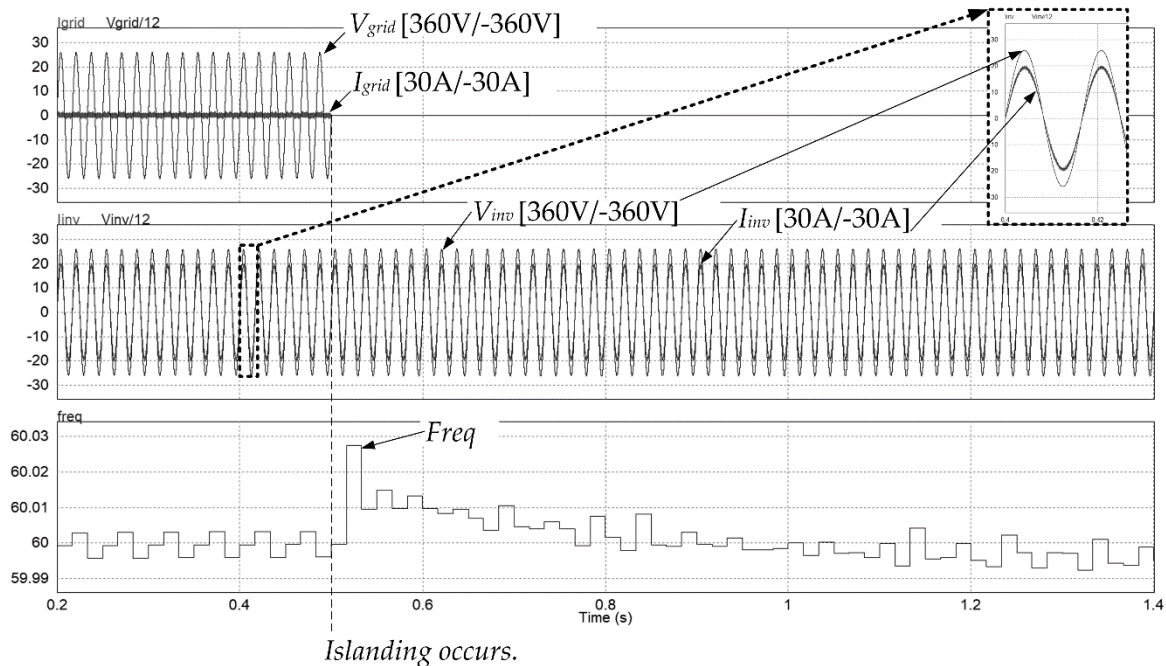


Figure 7. Islanding test results when no anti-islanding method is used.

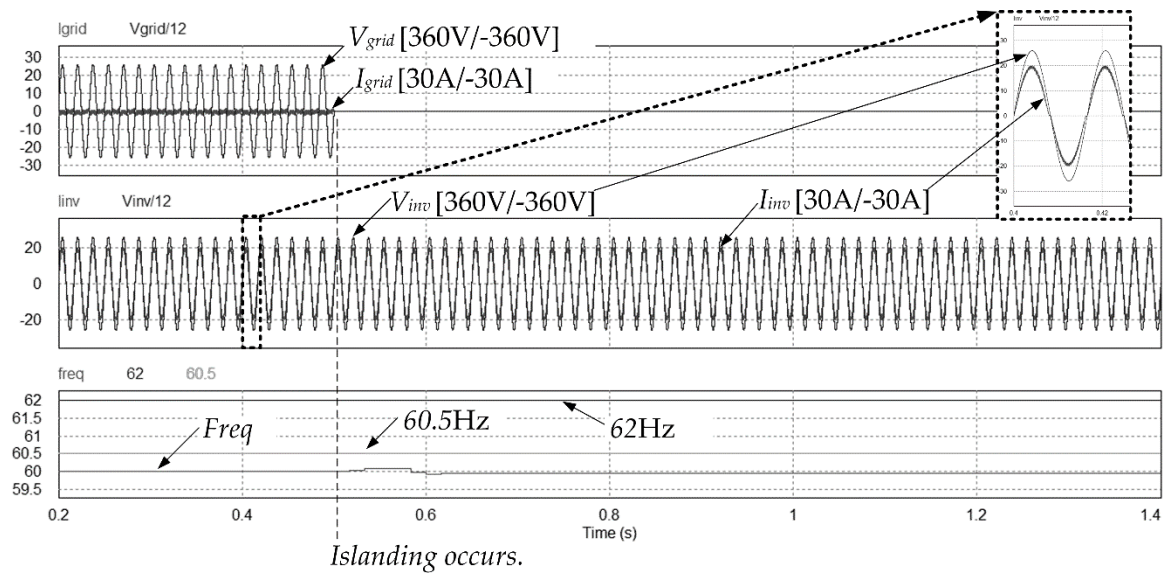


Figure 8. Anti-islanding test results when active frequency drift method ($cf = 5\%$) is used.

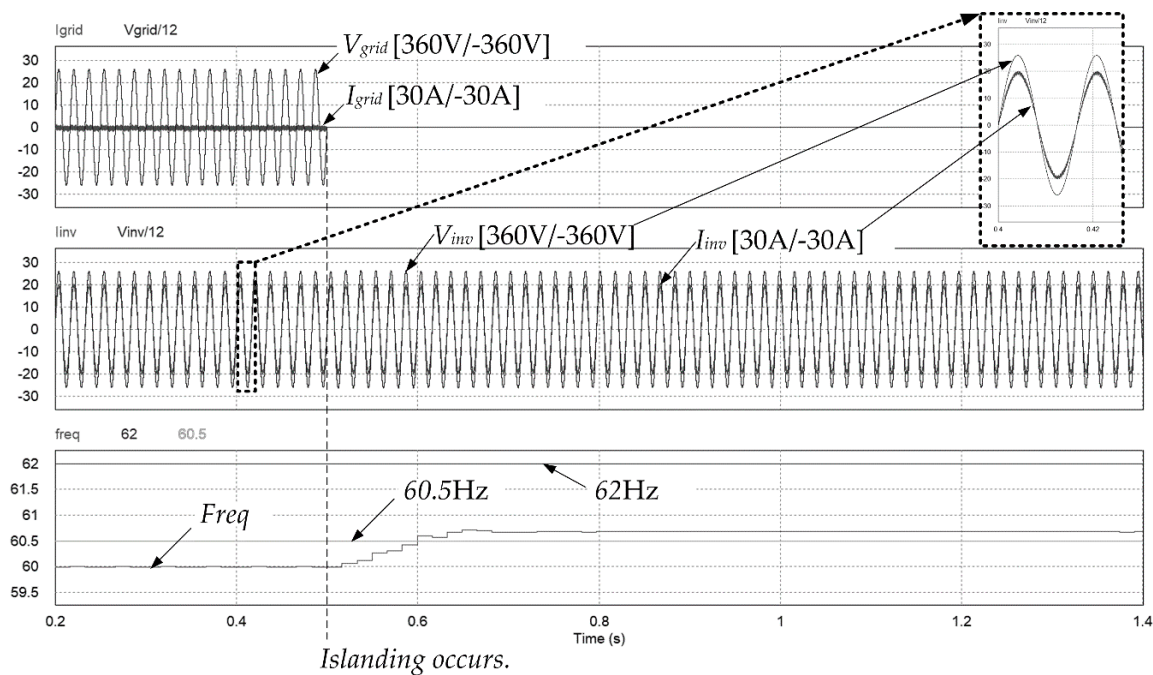


Figure 9. Anti-islanding test results when active frequency drift method with positive feedback is used.

The simulation results are summarized in Table 3. When the grid is connected to DG, the THD_i values of AIM methods are assessed. In the conventional AFD method, THD_i increases to 5.53% as the cf value increases from 1% to 5%. Both the AFDPF method and the proposed method show low THD_i , which is 3.18%, because the initial value cf 1% is only inserted when the grid is connected. For AFD method, islanding is not prevented because DG source and load power were balanced. For AFDPF method, islanding is also not prevented, because the frequency deviation is not enough by using low K_p gain 0.02. In case of the proposed method, islanding is prevented with the same K_p gain of AFDPF method, because this method does not depend on the frequency trip settings.

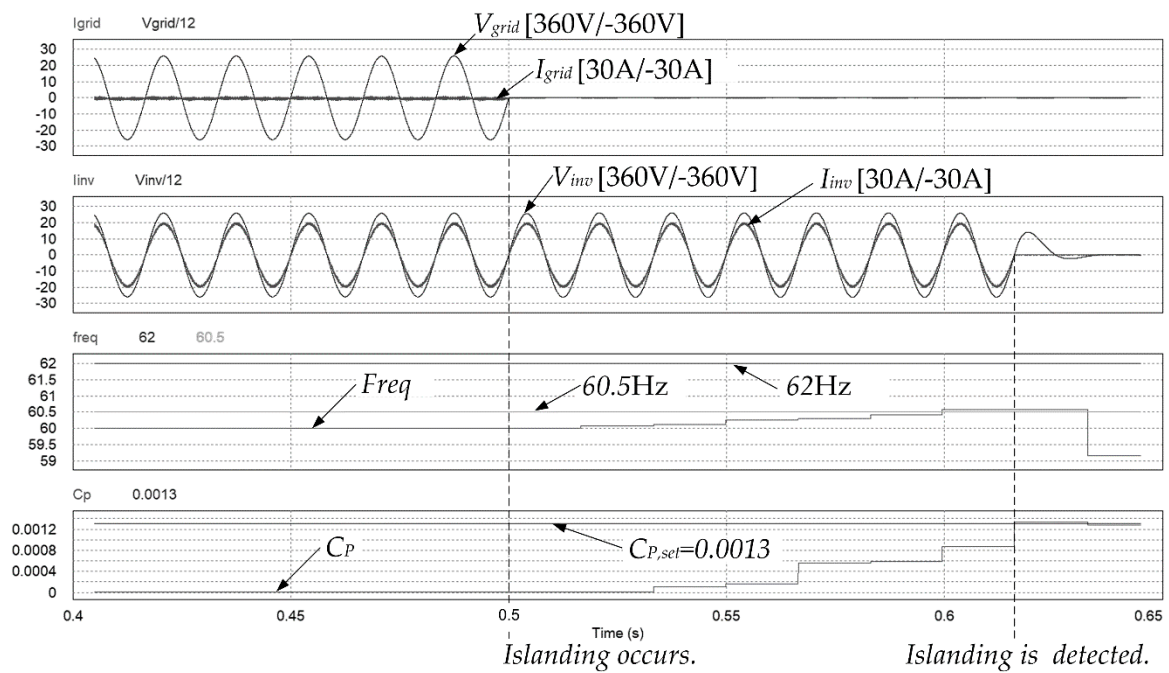


Figure 10. Anti-islanding test results when the proposed method is used.

Table 3. Performance comparison among AIMS.

Parameter \ AIM	AFD Method (Fixed cf)					AFDPF Method (Varying cf)	The Proposed Method (Varying cf)
cf [%]	1	2	3	4	5	$cf[k] = cf[k - 1] + K_p(Freq[k] - Freq[k - 1])$	
K_p	- (No need)					0.02	0.02
Anti-islanding detection time [s] at ΔP and $\Delta Q \approx 0$	No detection					No detection	0.116
THD_i [%] before islanding	3.18	3.19	3.53	4.10	5.53	3.18	3.18

5. Conclusions

This paper presents a correlation-based AIM under wider frequency trip settings for DG. Since a significant loss of DG due to a short disturbance could cause another reliability issue for an EPS, wider frequency trip settings were introduced in IEEE Std. 1547–2018. Under these conditions, the conventional AIM might not detect islanding with lower current distortion. Thus, the proposed method presents an islanding detection indicator as the correlation parameter between current disturbance and the corresponding frequency, and shows high islanding-detection capability with less current distortion through simulation results. According to the simulation results, the proposed AIM method detects islanding under the IEEE Std. 1547–2018 test condition within 2 s, which meets the standard requirement, and it has around 3.18% THD_i , which is relatively lower compared with the conventional AFD method having 5% cf .

Funding: This work was supported by the National Research Foundation of Korea (NRF) grant funded by the Korea government (MSIP) [grant number 2019R1H1A1080039].

Conflicts of Interest: The authors declare no conflicts of interest.

References

- Chen, G.; Lewis, F.L.; Feng, E.N.; Song, Y. Distributed optimal active power control of multiple generation systems. *IEEE Trans. Ind. Electron.* **2015**, *62*, 7079–7090. [CrossRef]
- Huang, W.; Zhang, N.; Yang, J.; Wang, Y.; Kang, C. Optimal Configuration Planning of Multi-Energy Systems Considering Distributed Renewable Energy. *IEEE Trans. Smart Grid* **2019**, *10*, 1452–1464. [CrossRef]
- Cady, S.T.; Dominguez-Garcia, A.D.; Hadjicostis, C.N. A distributed generation control architecture for islanded AC microgrids. *IEEE Trans. Control. Syst. Technol.* **2015**, *23*, 1717–1735. [CrossRef]
- Tan, Y.; Wang, Z. Incorporating unbalanced operation constraints of three-phase distributed generation. *IEEE Trans. Power Syst.* **2019**, *34*, 2449–2452. [CrossRef]
- Massignan, J.A.D.; Pereira, B.R.; London, J.B.A. Load flow calculation with voltage regulators bidirectional mode and distributed generation. *IEEE Trans. Power Sys.* **2017**, *32*, 1576–1577.
- Makwana, Y.M.; Bhalja, B.R. Experimental Performance of an Islanding Detection Scheme Based on Modal Components. *IEEE Trans. Smart Grid.* **2019**, *10*, 1025–1035. [CrossRef]
- Raipala, O.; Makinen, A.S.; Jarventrausta, P. An anti-islanding protection method based on reactive power injection and ROCOF. *IEEE Trans. Power Deliv.* **2017**, *32*, 401–410. [CrossRef]
- IEEE Standard for Interconnection and Interoperability of Distributed Energy Resources with Associated Electric Power Systems Interfaces*; IEEE Std. 1547–2018; IEEE Standard Association: Piscataway, NJ, USA, 2018.
- Recommended Settings for Voltage and Frequency Ride-Through of Distributed Energy Resources. EPRI Report, Product Id: 3002006203. Available online: <https://www.epri.com/#/pages/product/3002006203/> (accessed on 25 April 2020).
- Pouryekta, A.; Ramachandaramurthy, V.K.; Mithulananthan, N.; Arulampalam, A. Islanding Detection and Enhancement of Microgrid Performance. *IEEE Syst. J.* **2018**, *12*, 3131–3141.
- Liu, S.; Zhuang, S.; Xu, Q.; Xiao, J. Improved voltage shift islanding detection method for multi-inverter grid-connected photovoltaic systems. *IET Gener. Transm. Distrib.* **2016**, *10*, 3163–3169. [CrossRef]
- Guha, B.; Haddad, R.J.; Kalaani, Y. Voltage ripple-based passive islanding detection technique for grid-connected photovoltaic inverters. *IEEE Power Energy Technol. Syst. J.* **2016**, *3*, 143–154. [CrossRef]
- Raza, S.; Mokhlis, H.; Arof, H.; Laghari, A.; Mohamad, H. A sensitivity analysis of different power system parameters on islanding detection. *IEEE Trans. Sustain. Energy* **2016**, *7*, 461–470. [CrossRef]
- Liu, N.; Diduch, C.; Chang, L.; Su, J. A reference impedance-based passive islanding detection method for inverter-based distributed generation system. *IEEE J. Emerg. Sel. Top. Power Electron.* **2015**, *3*, 1205–1217. [CrossRef]
- Kim, B.; Sul, S. Stability-Oriented Design of Frequency Drift Anti-Islanding and Phase-Locked Loop Under Weak Grid. *IEEE J. Emerg. Sel. Top. Power Electron.* **2017**, *5*, 760–774. [CrossRef]
- Wen, B.; Boroyevich, D.; Burgos, R.; Shen, Z.; Mattavelli, P. Impedance-Based Analysis of Active Frequency Drift Islanding Detection for Grid-Tied Inverter System. *IEEE Trans. Ind. Appl.* **2016**, *52*, 332–341. [CrossRef]
- Pourbabak, H.; Kazemi, A. Islanding detection method based on a new approach to voltage phase angle of constant power inverters. *IET Gener. Transm. Dis.* **2016**, *10*, 1190–1198. [CrossRef]
- Chen, X.; Li, Y. An Islanding Detection Method for Inverter-Based Distributed Generators Based on the Reactive Power Disturbance. *IEEE Trans. Power Electron.* **2016**, *31*, 3559–3574. [CrossRef]
- Khan, M.A.; Kurukuru, V.S.B.; Haque, A.; Mekhilef, S. Islanding Classification Mechanism for Grid-Connected Photovoltaic Systems. *IEEE J. Emerg. Sel. Top. Power Electron.* **2020**. [CrossRef]
- Faqhruldin, O.N.; EL-Saadany, E.F.; Zeineldin, H.H. A universal islanding detection technique for distributed generation using pattern recognition. *IEEE Trans. Smart Grid.* **2014**, *5*, 1985–1992. [CrossRef]
- Yu, B. *An Improved Active Frequency Drift Anti-Islanding Detecting Module for Multiple PV Micro-Inverter Systems and Detecting Method Using the Same*; No. 10-1530207: Seoul, Korea, 2014.
- Ye, Z.; Kolwalkar, A.; Zhang, Y.; Du, P.; Walling, R. Evaluation of anti-islanding schemes based on nondetection zone concept. *IEEE Trans. Power Electron.* **2004**, *19*, 1171–1176. [CrossRef]
- Utility-Interconnected Photovoltaic Inverters-Test Procedure of Islanding Prevention Measures*; IEC 62116:2014; International Electrotechnical Commission: Geneva, Switzerland, 2014.
- Ropp, M.E.; Begovic, M.; Rohatgi, A. Analysis and performance assessment of the active frequency drift method of islanding prevention. *IEEE Trans. Energy Convers.* **1999**, *14*, 810–816. [CrossRef]

25. Vahedi, H.; Mehdi, K.; Gharehpetian, G.B. Accurate SFS Parameter Design Criterion for Inverter-Based Distributed Generation. *IEEE Trans. Power Deliv.* **2016**, *31*, 1050–1059. [[CrossRef](#)]
26. Sun, Q.; Guerrero, J.M.; Jing, T.; Vasquez, J.C.; Yang, R. An Islanding Detection Method by Using Frequency Positive Feedback Based on FLL for Single-Phase Microgrid. *IEEE Trans. Smart Grid.* **2017**, *8*, 1821–1830. [[CrossRef](#)]
27. Jung, Y.; Choi, J.; Yu, G. A novel active anti-islanding method for grid-connected photovoltaic inverter. *J. Power Electron.* **2007**, *7*, 64–71.
28. *IEEE Recommended Practice for Utility Interface of Photovoltaic (PV) Systems*; IEEE Std. 929-2000; IEEE Standard Association: Piscataway, NJ, USA, 2000.



© 2020 by the author. Licensee MDPI, Basel, Switzerland. This article is an open access article distributed under the terms and conditions of the Creative Commons Attribution (CC BY) license (<http://creativecommons.org/licenses/by/4.0/>).